Tunneling through triple quantum dots with mirror symmetry

T. Kuzmenko,[1] K. Kikoin,[2] and Y. Avishai[2,3,4]
[1]*The Rudolf Peierls Center for Theoretical Physics, University of Oxford, 1 Keble Road, Oxford OX1 3NP, United Kingdom*
[2]*Department of Physics, Ben-Gurion University of the Negev, Beer-Sheva 84105, Israel*
[3]*Ilse Katz Center for Nano-Technology, Ben-Gurion University of the Negev, Beer-Sheva 84105, Israel*
[4]*Department of Applied Physics, University of Tokyo, Hongo, Bunkyo-ku, Tokyo 113, Japan*
(Received 22 February 2006; revised manuscript received 23 April 2006; published 6 June 2006)

Indirect exchange interactions between itinerant electrons and nanostructures with nontrivial geometrical configurations manifest a plethora of unexpected results. These configurations can be realized either in quantum dots with several potential valleys or in real complex molecules with strong correlations. Here we demonstrate that the Kondo effect may be suppressed under certain conditions in triple quantum dots with mirror symmetry at odd electron occupation. First, we show that the indirect exchange has a ferromagnetic sign in the ground state of triple quantum dots in a two-terminal cross geometry for electron occupation $N=3$. Second, we show that for electron occupation $N=1$ in three-terminal fork geometry the zero-bias anomaly in the tunnel conductance is absent (despite the presence of Kondo screening) due to the special symmetry of the dot wave function.

DOI: 10.1103/PhysRevB.73.235310 PACS number(s): 72.10.−d, 72.15.−v, 73.63.−b

I. INTRODUCTION

Many-particle effects in quantum tunneling through quantum dots are extensively discussed in the current literature (see, e.g., the recent reviews in Refs. 1 and 2). Single-electron tunneling under the conditions of a strong Coulomb blockade is accompanied by cotunneling processes with spin reversal, which involve dynamical screening effects similar to the celebrated Kondo scattering in magnetically doped metals. The pertinent effect was predicted and observed in single-well quantum dots with odd electron occupation, where the electrons confined in the well are represented by the non compensated spin 1/2 of an electron on the highest occupied discrete level. This generic pattern may be enriched in many ways, in particular by studying tunneling through complex quantum dots containing two or three valleys.

In this paper we are interested in specific physical properties of electron tunneling through complex quantum dots containing several potential valleys with essentially different capacitances. Originally, the idea of coupling several nano-objects having strong and weak Coulomb interactions is formulated in the context of the electron and spin structure of complex molecules (e.g., lantanocenes, containing strongly correlated f electrons hybridized with weakly correlated molecular orbitals occupied by p electrons). It is noticed[3] that the energy difference between the singlet (S) ground state and triplet (T) excited state of a molecule with even number of electrons $N=N_f+N_p$ is anomalously small, so that triplet excitation affects the magnetic response of the system. The simplest artificial analog of this system is an asymmetric double quantum dot (composed of large and small dots) with even occupation (e.g., $N=2$) and charging energies $Q_s \gg Q_l$ for small and large dots, respectively. When this double quantum dot is coupled with metallic leads via the large dot (the T-shaped geometry), then lead-dot electron tunneling may induce an $S \rightarrow T$ crossover[4] when the energy E_T of the triplet state becomes lower than the energy E_S of the singlet state. In the case of odd occupation $N=1$, the Kondo-Fano regime is relevant, where the Kondo effect induced by an electron localized in the small side dot affects the electron tunneling through the weakly correlated large dot.[5] If the leads are connected via the small dot, the large dot plays the role of additional reservoir for Kondo screening in the case of odd N and the two-channel Kondo effect may be realized under certain conditions.[6,7]

A more complicated model of the asymmetric triple quantum dot (TQD) with a small dot sandwiched between two large dots was considered in Ref. 8 for odd and even occupations $N=3,4$. It was shown that the Kondo regime is accessible in both cases. Moreover, the TQD with even occupation demonstrates SO(n) symmetry.

Recently, a mirror symmetric TQD (see Fig. 1) in an "open" regime (near the Coulomb blockade peak) was studied both experimentally[9] and theoretically.[10] In this case the large "mesoscopic" dot is connected with two small dots and with metallic reservoirs. As a result, an indirect RKKY exchange interaction between the spins in the couple of small dots occurs and its sign may be controlled by changing the parameters of the large central dot by applying an external magnetic field.

Here we focus on a mirror-symmetric TQD in the "closed" regime—that is, the valley between Coulomb-

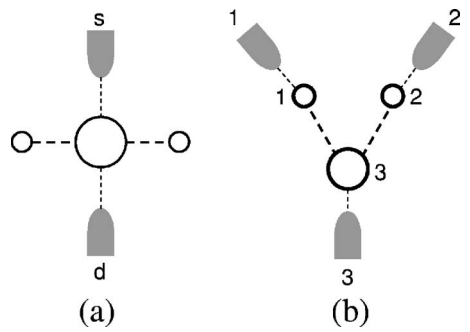

FIG. 1. Triple quantum dots in "cross" (a) and "fork" (b) geometries.

blockade peaks where the total number of electrons in the TQD is fixed. The three valleys of the TQD are coupled both by capacitive interaction and by tunneling channels. Our main results are that (i) in the cross geometry [Fig. 1(a)] with electron occupation $N=3$, such a dot possesses an unusual property—*the indirect exchange tunneling constant between the large dot and the leads is ferromagnetic*; the Kondo tunneling is therefore absent although the TQD behaves as a local moment; (ii) in a "fork" configuration [Fig. 1(b)] with electron occupation $N=1$, the TQD exhibits two different tunneling regimes: depending on the gate voltages, the Kondo regime may be observed as a zero-bias anomaly or as a finite-bias anomaly in the tunnel conductance.

II. TRIPLE QUANTUM DOT IN A CROSS GEOMETRY

The TQD in the cross geometry [Fig. 1(a)] is composed of left l, center c, and right r dots, with corresponding levels and charging energies $\epsilon_j, Q_j, j=l,c,r$. It is modeled by the Anderson Hamiltonian

$$H = H_d + H_{lead} + H_t, \tag{1}$$

containing the terms describing the dot, two leads, and dot-lead tunneling, respectively. The first term is

$$H_d = \sum_{j=l,c,r} \sum_{\sigma} \epsilon_j d_{j\sigma}^{\dagger} d_{j\sigma} + \sum_j Q_j n_{j\uparrow} n_{j\downarrow} + W \sum_{j=l,r} \sum_{\sigma} (d_{j\sigma}^{\dagger} d_{c\sigma} + \text{H.c.}). \tag{2}$$

The parameters Q_j are chosen in such a way that for electron occupation $N=3$ and in the absence of interdot tunneling ($W=0$), each dot is occupied by one electron. In the mirror-symmetric case such configuration is realizable provided

$$\epsilon_l = \epsilon_r \equiv \epsilon_s, \quad \Delta = \epsilon_c - \epsilon_s > 0,$$

$$Q_l = Q_r \equiv Q_s \gg Q_c. \tag{3}$$

We do not take into consideration the interdot capacitive interaction Q_{jc} (which may arise provided both central and side dots are in charged states), because this interaction merely results in certain level shifts, which are not relevant for the effects under consideration. At finite interdot tunneling strength W, charge transfer from the central dot to the side dots is possible, but the double occupation of the side valleys is still suppressed by a strong Coulomb blockade ($Q_s \gg W$). In the charge sector $N=3$ and for the mirror-symmetric configuration the lowest-energy states are two spin doublets (even and odd relative to the $l \leftrightarrow r$ permutation), a spin quartet state, and a doubly degenerate charge-transfer exciton (with two electrons in the central dot). The corresponding energies are

$$E_{Du} = 2\epsilon_s + \epsilon_c - 3W^2/\Delta',$$

$$E_{Dg} = 2\epsilon_s + \epsilon_c - W^2/\Delta',$$

$$E_Q = 2\epsilon_s + \epsilon_c,$$

$$E_{Ex} = \epsilon_s + 2\epsilon_c + Q_c + 2W^2/\Delta'. \tag{4}$$

Here $\Delta' = \Delta + Q_c$ and the inequality $W/\Delta' \ll 1$ is assumed to be valid. The eigenfunctions of the doublet and quartet states (which predetermine the structure of the effective exchange Hamiltonian; see below) are

$$|D_u\sigma\rangle = \left[\cos\theta_u \frac{(b_{cr}^{\dagger} d_{l\sigma}^{\dagger} - b_{cl}^{\dagger} d_{r\sigma}^{\dagger})}{\sqrt{3}} + \sin\theta_u b_{cc}^{\dagger}(d_{l\sigma}^{\dagger} - d_{r\sigma}^{\dagger})\right]|0\rangle,$$

$$|D_g\sigma\rangle = \left[\cos\theta_g b_{lr}^{\dagger} d_{c\sigma}^{\dagger} - \sin\theta_g b_{cc}^{\dagger}(d_{l\sigma}^{\dagger} + d_{r\sigma}^{\dagger})\right]|0\rangle,$$

$$\left|Q, +\frac{3}{2}\right\rangle = d_{l\uparrow}^{\dagger} d_{c\uparrow}^{\dagger} d_{r\uparrow}^{\dagger}|0, \quad \left|Q, -\frac{3}{2}\right\rangle = d_{l\downarrow}^{\dagger} d_{c\downarrow}^{\dagger} d_{r\downarrow}^{\dagger}|0\rangle,$$

$$\left|Q, +\frac{1}{2}\right\rangle = \frac{1}{\sqrt{3}} \sum_{\langle ijk\rangle} d_{i\uparrow}^{\dagger} d_{j\uparrow}^{\dagger} d_{k\downarrow}^{\dagger}|0\rangle,$$

$$\left|Q, -\frac{1}{2}\right\rangle = \frac{1}{\sqrt{3}} \sum_{\langle ijk\rangle} d_{i\downarrow}^{\dagger} d_{j\downarrow}^{\dagger} d_{k\uparrow}^{\dagger}|0\rangle. \tag{5}$$

Here $b_{ij}^{\dagger} = [d_{i\uparrow}^{\dagger} d_{j\downarrow}^{\dagger} - d_{i\downarrow}^{\dagger} d_{j\uparrow}^{\dagger}(1-\delta_{ij})]/\sqrt{2}$ and the rotation angles are given by $\theta_u = \arcsin(\sqrt{3}W/\Delta')$ and $\theta_g = \arcsin(W/\Delta')$.

The two other terms in Eq. (1) are the band Hamiltonian describing the electrons in the leads,

$$H_{lead} = \sum_{a=s,d} \sum_{k\sigma} \epsilon_{ak} c_{ak\sigma}^{\dagger} c_{ak\sigma}, \tag{6}$$

and the tunneling Hamiltonian

$$H_t = \sum_{ak\sigma} (V_a c_{ak\sigma}^{\dagger} d_{c\sigma} + \text{H.c.}). \tag{7}$$

Following the standard procedure, one derives an indirect exchange interaction between lead and dot electrons by means of the Schrieffer-Wolff (SW) transformation. For a composite quantum dot, this is accomplished in terms of spin eigenstates of H_d defined in Eqs. (4) and (5).

Thus, in the SW regime the main contribution to the lead-dot tunneling is given by the components $\sim\cos\theta_{g,u}$. The quartet state has the usual structure prescribed by a standard Young tableau for three electrons ($\langle ijk\rangle$ indicates the cyclic permutation of three sites lcr).

After performing the SW-like canonical transformation, one gets the effective exchange Hamiltonian

$$H_{ex} = J_u \mathbf{S}_u \cdot \mathbf{s}, \tag{8}$$

where $\mathbf{S}_u$ is the spin-1/2 vector operator with components $S_u^+ = |u\uparrow\rangle\langle u\downarrow|$ and $S_u^z = (|u\uparrow\rangle\langle u\uparrow| - |u\downarrow\rangle\langle u\downarrow|)/2$ and $\mathbf{s}$ is the spin operator of lead electrons defined as $\mathbf{s} = \Sigma_k c_{ek\sigma}^{\dagger} \hat{\tau} c_{ek\sigma'}$; $\hat{\tau}$ is the set of Pauli matrices, and $c_{e\sigma}$ is the even combination of lead electron annihilation operators (the odd one is excluded from the tunneling Hamiltonian by standard rotation[11]). Remarkably, the exchange constant J_u has a *ferromagnetic* sign,

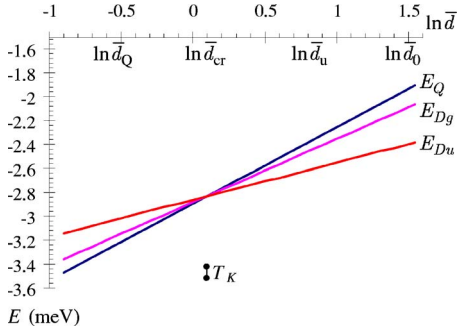

FIG. 2. (Color online) Haldane flow diagram for the levels E_Λ of Eq. (10), $\bar{d}=\pi\bar{D}/\Gamma_Q$. Energy is measured in meV units.

$$J_u = -\frac{2\cos^2\theta_u V^2}{3}\left(\frac{1}{|\epsilon_c|}+\frac{1}{|\epsilon_c+Q_c|}\right) \tag{9}$$

($|\epsilon_c|$ is the position of the central dot level relative to the Fermi energy of the leads; source and drain contacts are assumed to be equivalent, $V_s=V_d=V$). The reason for an unconventional sign of the exchange interaction is that only one of three electrons in the TQD is involved in an exchange interaction with the leads, and the overlap of the two other electrons wave function entering the state $|D_u\sigma\rangle$ gives the factor -1. Thus, in this geometry we encounter a unique situation, where the Kondo screening is ineffective for a quantum dot with *odd occupation*.

Yet a crossover from a ferromagnetic to an antiferromagnetic scenario is feasible. Indeed, the level spacing in the spin multiplet (4) is governed by the parameter W/Δ. If this spacing is small enough, the renormalization of these levels due to lead-dot cotunneling becomes relevant in the renormalization group (RG) flow equations along with exchange screening in the framework of the Haldane renormalization procedure.[12] Accordingly, the energy levels (4) are renormalized as a result of integrating out the band edges and shrinking the bandwidth from its bare value D_0 to a smaller value D (comparable with $|\epsilon_c|$). The corresponding RG invariant is

$$E_\Lambda^* = E_\Lambda(D) - \pi^{-1}\Gamma_\Lambda \ln(\pi D/\Gamma_\Lambda), \tag{10}$$

with tunneling rates $\Gamma_{D(u,g)} \approx \pi\rho_0\cos^2\theta_{(u,g)}V^2$ and $\Gamma_Q \approx \pi\rho_0 V^2$. Due to the hierarchy $\Gamma_Q > \Gamma_{Dg} > \Gamma_{Du}$, a level crossing is feasible (see Fig. 2). Physically, it implies a crossover from the non-Kondo (ferromagnetic exchange) regime to the underscreened Kondo regime with a pronounced maximum of the conductance around the degeneracy point. The parameters W and Δ, which determine the initial conditions (4) for the flow equations (10), can be controlled by gate voltages. Varying these initial conditions, one may tune the region of crossover to the SW regime at the point

$$\bar{D} \approx E_\Lambda(\bar{D}). \tag{11}$$

For $D<\bar{D}$ the properties of the system are determined by the SW Hamiltonian. The effective Hamiltonian (8) may be written for $\bar{D}=\bar{D}_u$ (marked on the horizontal axis of Fig. 2). If the condition (11) is fulfilled in the vicinity of the crossing point ($\bar{D}=\bar{D}_{cr}$), the exchange Hamiltonian [instead of Eq. (8)] acquires the form

$$H_{SW} = J_u\mathbf{S}_u\cdot\mathbf{s} + J_g\mathbf{S}_g\cdot\mathbf{s} + J_Q\mathbf{S}_Q\cdot\mathbf{s} + J_R\mathbf{R}\cdot\mathbf{s}, \tag{12}$$

expressed in terms of operators for localized spin 1/2, $\mathbf{S}_{u,g}$, the quartet spin-3/2 operator $\mathbf{S}_Q$, and the vector operator $\mathbf{R}$ which induces transitions between the quartet $|Q\rangle$ and doublet $|D_u\rangle$. There are no transitions between $|Q\rangle$ and $|D_g\rangle$ since these states have different $l-r$ parity.

At the point $\bar{D}_{cr}$ the degeneracy of the spin state of the TQD is maximal, corresponding to the symmetry SU(2) $\times$ SU(2) $\times$ SU(2). Both to the right and to the left of this point some of the states in the spin multiplets are quenched at $T\to T_K$ and T_K depends on the energy gaps $\Delta_{Qg}=E_Q(\bar{D})-E_{Dg}(\bar{D})$ and $\Delta_{gu}=E_{Dg}(\bar{D})-E_{Du}(\bar{D})$. To find the function $T_K(\Delta_{Qg},\Delta_{gu})$, one should solve the scaling equations for the coupling constants in the Hamiltonian H_{SW},

$$\frac{dj_u}{d\ln d} = -[j_u^2+2j_R^2], \quad \frac{dj_g}{d\ln d} = -j_g^2,$$

$$\frac{dj_Q}{d\ln d} = -[j_Q^2-j_R^2], \quad \frac{dj_R}{d\ln d} = -\frac{j_R}{4}(5j_Q-j_u), \tag{13}$$

where $j_a=\rho_0 J_a$ ($a=g,u,Q,R$) and ρ_0 is the density of states which is assumed to be constant. The procedure is self-consistent because T_K itself predetermines the characteristic energy interval for states in the spin Hamiltonian involved in its formation. Varying $\bar{D}$ in Fig. 2, from the ferromagnetic non-Kondo regime ($\bar{D}\sim\bar{D}_u$) to the crossing point $\bar{D}_{cr}$, one reaches the point $T_K>0$ which arises due to influence of the excited states $E_Q(\bar{D})$ and $E_{Dg}(\bar{D})$. Just then, T_K sharply increases, reaching its maximum value in the point of maximum degeneracy, $\bar{D}_{cr}$. Moving further to the left, the level E_{Du} freezes out. This means that the vector $\mathbf{R}$ in the Hamiltonian (12) does not contribute anymore to Kondo cotunneling and the Kondo effect is determined by the pair of states E_Q and E_{Dg}, with the dynamical symmetry of TQD being SU(2) $\times$ SU(2). A further decrease of $\bar{D}$ eventually results in the quenching of E_{Dg}. The system then exhibits an underscreened Kondo regime of a localized spin-3/2 moment. Figure 3 illustrates these crossover effects on T_K.

The evolution of T_K is reflected in the behavior of the tunnel transparency and conductance as a function of energy. Far enough to the left and to the right of the crossing point, this behavior is stepwise. When the dot is in the doublet ground state ($\bar{D}\sim\bar{D}_u$), the spin multiplet as a whole contributes to the transparency at high energies $\omega\sim\Delta_{Qg}+\Delta_{gu}$. With decreasing ω the quartet E_Q and the even doublet E_{Dg} energies freeze out in this order (they are not renormalized anymore). Eventually, Kondo tunneling is quenched at low energies, so that the zero-bias anomaly (ZBA) has the shape of a dip. On the other hand, in the crossover regime, the ZBA follows the conventional Kondo peak. Finally, the structure of the peak at the regime $\bar{D}\sim\bar{D}_Q$ is even more complicated. Within the framework of our approach we may describe the

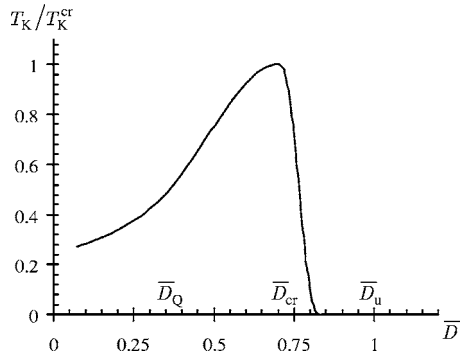

FIG. 3. Evolution of the Kondo temperature [(T_K^{cr} is determined by scaling equations (13)].

evolution of transparency for $T > T_K$ where it is approximately described by the simple relation $\mathcal{T}(\omega) \sim \ln^{-2}[T/T_K(\omega)]$. The resulting curve is shown in Fig. 4.

This type of nonuniversal behavior of T_K is known in the theory of strongly correlated quantum dots with *even* occupation, where the singlet-triplet level crossing usually occurs.[4,8,13] The novelty of the present scenario is that it is manifested in quantum dots with *odd* occupation where the absence of the Kondo effect occurs due to ferromagnetic exchange coupling with the localized spin doublet. The nonuniversality of T_K occurs as this ferromagnetic exchange competes with two antiferromagnetic exchange interactions (with doublet and quartet localized moments), so that, in some sense, one deals with a "three-stage" Kondo effect. Thus, we have completed our discussion pertaining to the cross-shaped TQD of Fig. 1(a).

III. TRIPLE QUANTUM DOT IN A FORK GEOMETRY

It is then natural to expect peculiar features of Kondo tunneling also in a mirror-symmetric TQD in the fork geometry [Fig. 1(b)] with $Q_{l,r} \gg Q_c$. The dots and leads are labeled 1,2,3, and each dot is attached to its own lead. In the case of $N=3$, the exchange coupling J_3 between the central dot and its adjacent lead is ferromagnetic in accordance with Eq. (9), whereas those for the two other (small) dots (J_1, J_2) are antiferromagnetic. Besides, there are also nondiagonal exchange couplings $J_{ij}=J_{ji}$. All these are coupled within a system of RG flow equations. A question now arises: is it possible to find a regime where the Kondo resonance arises only in dots 1,2, whereas dot 3 remains Kondo inactive?

To answer this question, we calculate T_K and G within the same scheme as in the preceding section for a system described by the Hamiltonian (1) with the tunneling term

$$H_t = \sum_{j=1}^{3} \sum_{k\sigma} (V_j c_{jk\sigma}^{\dagger} d_{j\sigma} + \text{H.c.}) \tag{14}$$

instead of Eq. (7). The effective exchange Hamiltonian of this system is obtained in the same way as Eq. (12). The mirror $l-r$ symmetry entails $V_1 = V_2 \neq V_3$. If the ground state consists of the odd-parity doublet E_{D_u}, the corresponding SW Hamiltonian has the form

$$H_{SW} = \sum_{i=1}^{3} J_i \mathbf{S} \cdot \mathbf{s}_i + J_{12} \mathbf{S} \cdot (\mathbf{s}_{12} + \mathbf{s}_{21}) + J_{13} \mathbf{S} \cdot (\mathbf{s}_{13} + \mathbf{s}_{31}) + J_{23} \mathbf{S} \cdot (\mathbf{s}_{23} + \mathbf{s}_{32}). \tag{15}$$

Here the exchange constant $J_3 < 0$ is the same as J_u, Eq. (9), whereas $J_{1,2} > 0$. For $\cos\theta_u \approx 1$, these constants are

$$J_1 = J_2 = \frac{4}{3} \frac{V_1^2}{|\epsilon_s|},$$

$$J_3 = -\frac{2}{3} \left(\frac{V_3^2}{|\epsilon_c|} + \frac{V_3^2}{|\epsilon_c + Q_c|} \right),$$

$$J_{12} = -\frac{3}{2} \frac{(V_1 W)^2}{(\epsilon_c + Q_c - \epsilon_s)^2 |\epsilon_s|},$$

$$J_{13} = J_{23} = -\frac{1}{4} \frac{W V_1 V_3}{\epsilon_c + Q_c - \epsilon_s} \left(\frac{1}{|\epsilon_s|} + \frac{1}{|\epsilon_c|} \right). \tag{16}$$

The system of RG flow equations for the Hamiltonian (15) now reads,

$$\frac{dj_1}{d\ln d} = -[j_1^2 + j_{13}^2 + j_{12}^2],$$

$$\frac{dj_3}{d\ln d} = -[j_3^2 + 2j_{13}^2],$$

$$\frac{dj_{12}}{d\ln d} = -2j_1 j_{12},$$

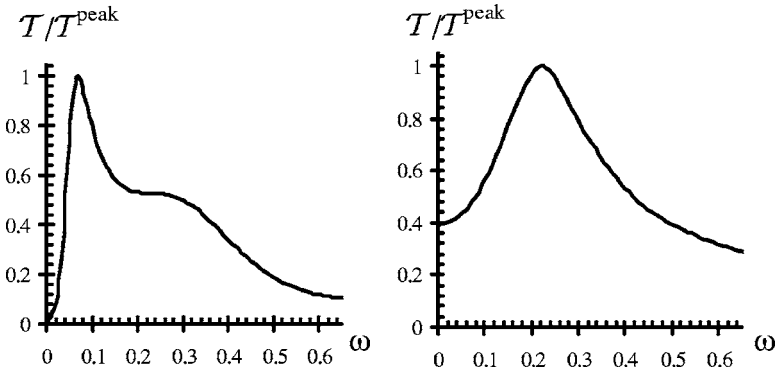

FIG. 4. Tunnel transparency of TQD in a doublet (left panel) and quartet (right panel) ground states. $\mathcal{T}_{peak}$ is the maximum value of $\mathcal{T}(\omega)$.

$$\frac{dj_{13}}{d\ln d} = -j_{13}(j_1 + j_3). \tag{17}$$

A somewhat unexpected result following the analysis of these equations: the coupling constants related to channel 3 become relevant in spite of their negative initial values (16). The Kondo temperature is

$$T_K = \bar{D}\exp\left(-\frac{2}{j_+ + \sqrt{j_-^2 + 6j_{13}^2}}\right), \tag{18}$$

where $j_+ = j_1 + j_{12} + j_3$ and $j_- = j_1 + j_{12} - j_3$, so that the Kondo resonance arises in all nondiagonal channels and the TQD looses its "exotic" properties. The Kondo transparency $\mathcal{T}_{ij}(\omega)$ may be calculated for any pair of electrodes (ij). It is a stepwise function in accordance with multistage Kondo screening process, but no anomalous "freezing out" of the Kondo effect similar to that shown in the left panel of Fig. 4 is expected in this case.

It is appealing, however, to exploit other specific properties of the TQD in the fork configuration. The remarkable feature of the mirror-symmetric TQD is that it can be viewed as a quantum pendulum.[14,15] This means that the superposition of two degenerate states (13) and (23) can be considered as a sort of mesoscopic resonating valence bond (RVB). In the two papers cited above, various manifestations of spin entanglement at even occupation $N=4,2$ were investigated. Below we will discuss how this property is manifested in the Kondo regime in the odd-occupation charge sector $N=1$.

So let us assume that the parameters (gate voltages) are tuned so that the TQD is found in a Coulomb-blockade valley corresponding to the occupation sector $N=1$. Within the same approximation as Eq. (4) the lowest eigenstates $|\Lambda\rangle$ of the Hamiltonian H_d, Eq. (2), for $N=1$ are the set of spin doublets

$$|Db\sigma\rangle = \left[\sin\theta d_{3\sigma}^\dagger + \cos\theta\frac{d_{1\sigma}^\dagger + d_{2\sigma}^\dagger}{\sqrt{2}}\right]|0\rangle,$$

$$|Dn\sigma\rangle = \left[\frac{d_{1\sigma}^\dagger - d_{2\sigma}^\dagger}{\sqrt{2}}\right]|0\rangle,$$

$$|Da\sigma\rangle = \left[-\cos\theta d_{3\sigma}^\dagger + \sin\theta\frac{d_{1\sigma}^\dagger + d_{2\sigma}^\dagger}{\sqrt{2}}\right]|0\rangle, \tag{19}$$

with $\sin\theta = \sqrt{2}W/\Delta \ll 1$. The corresponding eigenvalues are

$$E_{Db} = \epsilon_s - 2W^2/\Delta,$$

$$E_{Dn} = \epsilon_s,$$

$$E_{Da} = \epsilon_c + 2W^2/\Delta. \tag{20}$$

Hence, the ground state is a bonding spin doublet E_{Db} and the eigenstates $|\Lambda\rangle$ may be interpreted as two even and one odd RVB modes of a "spin pendulum."

In the low-energy subspace $\omega \ll W^2/\Delta$ the effective spin Hamiltonian which describes the Kondo cotunneling has the same form as Eq. (15) derived above for $N=3$. Here, however, all coupling constants are positive,

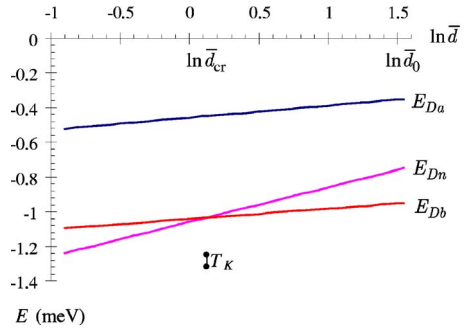

FIG. 5. (Color online) Haldane flow diagram for the levels E_Λ of the TQD in fork geometry, $\bar{d} = \pi\bar{D}/\Gamma_n$. Energy is measured in meV units.

$$J_1 = J_2 = J_{12} = \frac{V_1^2\cos^2\theta}{2|\epsilon_s|}, \quad J_3 = \frac{V_3^2\sin^2\theta}{|\epsilon_c|},$$

$$J_{13} = J_{23} = \frac{V_1V_3\sin\theta\cos\theta}{2\sqrt{2}}\left(\frac{1}{|\epsilon_c|} + \frac{1}{|\epsilon_s|}\right), \tag{21}$$

and the Kondo temperature is given by Eq. (18).

One may say that in a coherent Kondo-tunneling regime the system demonstrates perfect entanglement: an electron entering dot 3 from lead 3 splits into two components in accordance with the structure of the state $|Db\sigma\rangle$, and this entangled state predetermines the total current $I_1 + I_2$ through the TQD in the fork geometry. Of course, this statement is valid only at zero temperature and one may expect that thermal fluctuations are detrimental for a coherent transport, but this effect is suppressed as $(T/T_K)^2$ at low T.

The situation becomes even richer, due to the occurrence of soft mode excitations (20): the odd state $|Dn\sigma\rangle$ may be intermixed with the even state $|Db\sigma\rangle$ due to the cotunneling process. This intermixing becomes relevant provided $T_K \lesssim E_{Dn} - E_{Da}$. This inequality is, of course, invalid for the bare eigenstates (20), but a Haldane renormalization of the spectrum similar to that described by Eq. (10) may result in a softening of this mode. It might even lead to a level crossing provided the tunneling rate $\Gamma_n = \rho_1 V_1^2$ for the nonbonding state $|Dn\sigma\rangle$ is higher than the rate $\Gamma_b = \rho_1 V_1^2\cos^2\theta + \rho_3 V_3^2\sin^2\theta$ for the bonding state $|Db\sigma\rangle$. If the densities of states are the same in all leads, $\rho_1 = \rho_3$, then the condition $\Gamma_n > \Gamma_b$ means $V_1 > V_3$. The RG flow trajectories for this case are presented in Fig. 5. Like in the cross geometry, the TQD acquires an additional degeneracy in the critical region $\bar{d} \sim \bar{d}_{cr}$. However, in this case the sources of degeneracy are the RVB degrees of freedom. As a result, one encounters the problem of the Kondo effect due to an interplay between spin $\mathbf{S}$ and pseudospin $\boldsymbol{\mathcal{T}}$, where the latter describes the pendulum degrees of freedom. This problem was discussed in the context of double quantum dots,[16] triple quantum dots,[17,18] and molecular trimers chemisorbed on metallic surfaces.[19] In this case the actual symmetry of the TQD is SU(4). To show this, we derive below the effective spin Hamiltonian following the method offered in Ref. 18.

It is useful to generalize the notion of localized spin operator $S^i=|\sigma\rangle\hat{\tau}_i\langle\sigma'|$ [employing Pauli matrices $\hat{\tau}_i(i=x,y,z)$] to $S^i_{\Lambda\Lambda'}=|\sigma\Lambda\rangle\hat{\tau}_i\langle\sigma'\Lambda'|$, in terms of the eigenvectors $|Db\sigma\rangle,|Dn\sigma\rangle$ from Eqs. (19). A similar generalization applies for the spin operators of the lead electrons: $s^i_{\lambda\lambda'}=\Sigma_{\mathbf{k}\mathbf{k}'}c^\dagger_{\lambda,\mathbf{k}\sigma}\hat{\tau}_i c_{\lambda',\mathbf{k}'\sigma'}$. Here the index λ denotes conduction electrons in lead 3 ($\lambda=3$) and in leads 1,2, with $\lambda=e,o$ corresponding to even and odd combinations of conduction electron states in these leads,

$$c^\dagger_{(e,o)\mathbf{k}\sigma}=\frac{1}{\sqrt{2}}(c^\dagger_{1,\mathbf{k}\sigma}\pm c^\dagger_{2,\mathbf{k}\sigma}). \tag{22}$$

The pseudospin operators $\boldsymbol{\mathcal{T}}$ describing the RVB mode are introduced as follows:

$$\mathcal{T}^+=\sum_\sigma |Db\sigma\rangle\langle Dn\sigma|,\quad \mathcal{T}^-=[\mathcal{T}^+]^\dagger,$$

$$\mathcal{T}^z=\frac{1}{2}\sum_\sigma \left(|Db\sigma\rangle\langle Db\sigma|-|Dn\sigma\rangle\langle Dn\sigma|\right). \tag{23}$$

The five vector operators $\mathbf{S}_{\Lambda\Lambda'}$ and $\boldsymbol{\mathcal{T}}$ constitute the 15 generators of the SU(4) group.

Similarly, one may construct the pseudospin operators for the electrons in the leads (1,2):

$$\tau^+=\sum_{k\sigma} c^\dagger_{ek\sigma}c_{ok\sigma},\quad \tau^-=[\tau^+]^\dagger,$$

$$\tau_z=\frac{1}{2}\sum_{k\sigma}(c^\dagger_{ek\sigma}c_{ek\sigma}-c^\dagger_{ok\sigma}c_{ok\sigma}). \tag{24}$$

The exchange Hamiltonian for a TQD with spin and RVB degrees of freedom is

$$H_{SW}=\sum_{\kappa\lambda\mu\rho} J_{\kappa\lambda\mu\rho}\mathbf{S}_{\kappa\lambda}\cdot\mathbf{s}_{\mu\rho}+J_p\boldsymbol{\mathcal{T}}\cdot\tau, \tag{25}$$

with $\kappa,\lambda=b,n$; $\mu,\rho=e,o$, and the coupling constants $J_{\kappa\lambda\mu\rho}=J_{\lambda\kappa\mu\rho}=J_{\kappa\lambda\rho\mu}$ are positive like in Eqs. (21):

$$J_{bbee}=2J_{11},\quad J_{bb33}=J_{33},$$

$$J_{bnoe}=\frac{V_1^2\cos\theta}{|\epsilon_s|},\quad J_{nnoo}=\frac{V_1^2}{|\epsilon_s|},$$

$$J_{bb3e}=J_{13},\quad J_p=2J_{bbee}. \tag{26}$$

The system of scaling equations has the form

$$\frac{dj_b}{d\ln d}=-\left[j_b^2+\frac{j_{bn}^2}{2}+j_{bn}j_p+j_{13}^2\right],$$

$$\frac{dj_n}{d\ln d}=-\left[j_n^2+\frac{j_{bn}^2}{2}+j_{bn}j_p\right],$$

$$\frac{dj_3}{d\ln d}=-\left[j_3^2+j_{13}^2\right],$$

$$\frac{dj_{13}}{d\ln d}=-j_{13}(j_b+j_3),$$

$$\frac{dj_{bn}}{d\ln d}=-\frac{1}{2}(j_{bn}+j_p)(j_b+j_n),$$

$$\frac{dj_p}{d\ln d}=-j_p^2, \tag{27}$$

where $j_b=j_{bbee}$, $j_n=j_{nnoo}$, $j_3=j_{bb33}$, $j_{13}=j_{bb3e}$, and $j_{bn}=j_{bnoe}$. From these equations we derive the Kondo temperature

$$T_K=\bar{D}\exp\left\{-\frac{2}{j_+ +\sqrt{6j_{13}^2+(j_{bn}+j_p)^2+j_-^2}}\right\}, \tag{28}$$

with $j_+=j_b+j_n+j_3$ and $j_-=j_b-j_n-j_3$. Like in the cross geometry, one may manipulate $\bar{D}$ by changing the gate voltages and scanning the dependence $T_K(\bar{D})$ similarly to Fig. 3. This curve has a maximum in the critical point $\bar{D}_{cr}$, and the orbital degrees of freedom are frozen out in the asymptotic regimes $\bar{D}\gg\bar{D}_{cr}$ and $\bar{D}\ll\bar{D}_{cr}$. We deal in this case with a symmetry crossover $\mathrm{SU}(2)\to\mathrm{SU}(4)\to\mathrm{SU}(2)$. However, there is an important difference between the two asymptotic SU(2) symmetries.

In the limit $\bar{d}\gg\bar{d}_{cr}$ the ground state is E_{db}; all three dots are partially occupied in accordance with the structure of the corresponding wave function $|Db\sigma\rangle$, Eqs. (19). The terms $\sim J_{bbee}$, J_{bb33}, and J_{bb3e} survive in the SW Hamiltonian (25), and Eq. (28) for T_K reduces to Eq. (18). In the limit $\bar{d}\ll\bar{d}_{cr}$, the ground state of the TQD is the nonbonding state E_{Dn} with an empty site 3 in accordance with the form of the wave function $|Dn\sigma\rangle$, Eqs. (19). The SW Hamiltonian (25) contains in this case only the term $\sim J_{nnoo}$ and $T_K=\bar{D}\exp(-1/j_n)$.

The Kondo temperature as a function of $\bar{D}$ has a maximum in a crossing point $\bar{D}_{cr}$, but unlike the case of cross geometry (Fig. 3), $T_K(\bar{D})$ is nonzero on both sides of this maximum (Fig. 6).

The change of the ground-state wave function from the bonding combination $|D_{b\sigma}\rangle$ to the nonbonding one $|D_{n\sigma}\rangle$ influences the behavior of tunnel conductance. Let us compare the tunnel current between leads 2 and 1 and between leads 3 and 1, which is defined by the components G_{22} and G_{33} of the three-terminal conductance matrix $G_{ij}=\partial I_i/\partial V_j$.

When calculating these components as a function of $\bar{D}$, one immediately sees that the Kondo-type ZBA in G_{22} exists in all three regimes and the peak of this conductance follows the behavior of $T_K(\bar{D})$. The behavior of G_{33} is more peculiar. The ZBA in this channel exists only until the even components $|Db\sigma\rangle$ are involved in Kondo tunneling. In the limit $T_K\lesssim E_{Db}-E_{Dn}$ at $\bar{d}\ll\bar{d}_{cr}$ this anomaly disappears, so we encounter a unique situation where the Kondo resonance is absent in the conductance in spite of the presence of Kondo screening.

However, the resonance Kondo regime in G_{33} arises as a finite-bias anomaly (FBA). To describe this tunneling one

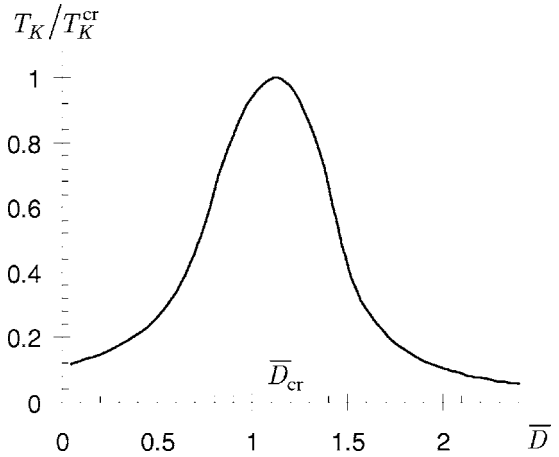

FIG. 6. Evolution of the Kondo temperature [(T_K^{cr} is determined by Eq. (28)].

has to retain the terms $\sim J_{bnoe}$ and J_p in the Hamiltonian (25). These terms describe *inelastic* tunneling, which acquires a form of Kondo resonance at finite bias in accordance with the mechanism offered in Ref. 20. In that case the tunneling through the double quantum dot with even occupation in a singlet ground state was considered and the Kondo regime becomes relevant at finite bias when the difference in the chemical potentials of source and drain leads compensates the exchange gap between the ground-state singlet and excited-spin triplet states. In our case the FBA arises at odd occupation when the bias compensates the energy gap, $\delta = E_{Db} - E_{Dn}$.

In order to calculate the tunnel conductance in the weak-coupling regime, we use the modified golden rule formula,[21] which reads for channel 3–1 as $G_{33}(eV_3,T)/G_0 \sim |\tilde{J}_{13}(eV_3,T)|^2$, where $G_0 = e^2/\pi\hbar$ and $\tilde{J}_{13}$ is the solution of the RG flow equations (27) for $D = \max\{eV_3, T\}$. In the case of Kondo-type resonance at finite bias eV_3, the equation for conductance in the vicinity of the FBA reads[20]

$$G/G_0 \sim \ln^{-2}(\max\{eV_3 - \delta, T\}/T_K). \tag{29}$$

A similar equation (with $V_2 \to 0$) describes the ZBA in tunnel conductance in channel 2–1.

The results of the calculation of G_{22} and G_{33} are presented in Fig. 7. One may see from this figure how the ZBA in G_{22} goes through the maximum at the crossing point $\bar{D}_{cr}$ whereas the ZBA in G_{33} transforms into the FBA for small enough $\bar{D}$ when δ exceeds T_K. Rough estimates of the boundaries of robustness of this effect in parameter space can be suggested as follows: let the small dots be not completely identical—i.e., $\epsilon_1 \neq \epsilon_2$, but $|\epsilon_1 - \epsilon_2| \ll \epsilon_c - \epsilon_s$. Then for $|\epsilon_1 - \epsilon_2| < |\frac{W^2}{\epsilon_c - \epsilon_s}|$, Eqs. (19) and (20) are valid, whereas for $|\epsilon_1 - \epsilon_2| > |\frac{W^2}{\epsilon_c - \epsilon_s}|$ all three eigenfunctions contain $d^\dagger_{3\sigma}|0>$ which means that the ZBA in G_{33} exists when the mirror symmetry is strongly violated.

A discussion of damping effects, which, to a certain degree, tend to smear the FBA,[20,22] is beyond the scope of this work. It should be mentioned, however, that it was shown in Ref. 20 that there exists a wide enough window of parameters where this damping is not fatal for the existence of a well-shaped FBA. It is worth noting also that the tunnel conductance between leads 1 and 2 exists in spite of the absence of direct tunneling channel. The tunneling mechanism is connected in this case with the "pendulum" structure of the electron wave function (19) in the TQD. In the case of the ground state E_{Db} this is the bonding combination $(d^\dagger_{1\sigma} + d^\dagger_{2\sigma})|0\rangle$; in the case of the ground state E_{Dn} this is the resonating valence bond $(d^\dagger_{1\sigma} - d^\dagger_{2\sigma})|0\rangle$. In the latter case dot 3 is excluded from cotunneling. It is therefore involved only in the determination of the Kondo temperature.

IV. CONCLUDING REMARKS

We have shown in this paper that triple quantum dots in some special geometries demonstrate unusual behavior in the Kondo tunneling regime. This behavior stems from the inequivalence of constituents (side valleys and central valley). The asymmetric double quantum dot considered in Ref. 4 was the first example of a complex quantum dot with inner and outer "shells." The trimers with inequivalent side and central valleys studied in Refs. 8–10 and in the present paper are more complicated examples of artificial molecules with shell structure. In this case the two side dots form an "inner shell" whereas the large central dot plays the role of an "outer shell." If the outer shell is open,[9,10] it contributes to the indirect exchange between the electrons in the inner shell.

In our theoretical model with closed geometry only the few-electron case was considered with electron occupation N up to 3. Of course, practical realizations of "nearly empty"

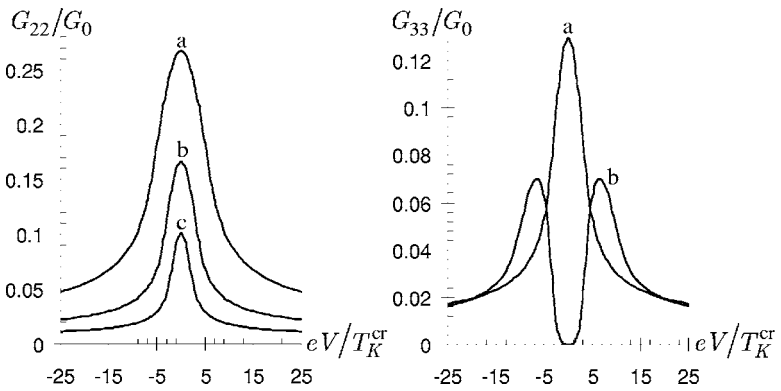

FIG. 7. Left panel: tunnel conductance in channel 2–1 for $\bar{D} = \bar{D}_{cr}$ (a), $\bar{D} > \bar{D}_{cr}$ (b), and $\bar{D} < \bar{D}_{cr}$ (c). Right panel: tunnel conductance in channel 3–1 for $\bar{D} > \bar{D}_{cr}$ (a) and $\bar{D} < \bar{D}_{cr}$ (b).

complex quantum dots is a difficult task. However, the standard condition for realization of the Kondo effect—namely, the smallness of tunnel parameters in comparison with the level spacing $\delta\varepsilon$ in the dots and strong Coulomb blockade, $W, V \ll \delta\varepsilon < Q_i$—is enough for realization of the physical effects described in this work. For example, the charge sector described here as the $N=1$ case corresponds to two side valleys occupied by an even number of electrons and the central sites occupied by an odd number of electrons. The case $N=3$ corresponds to odd occupation in all three valleys. If the above inequalities are valid, the spin excitations in these charge sectors are given by Eqs. (20) and (4), respectively. The experimental possibility of the observation of one excess electron at a time in triple quantum dots was demonstrated explicitly in studies of the ratchet effect.[23] Recently, the possibility of controlling quantum dots with a very small number of electrons ($N=1-20$) was experimentally realized.[27]

It should be stressed that the inequalities $\Delta > 0$ and $Q_s \gg Q_c$ are necessary preconditions for the "shell structure" of the electronic distribution in TQD's, mentioned in the beginning of this section. If the energy differences Δ and $Q_s - Q_c$ in the TQD are comparable with the interdot tunneling parameter W, the shell structure will be smeared and all specific features of the TQD related to the $l-r$ symmetry will be smeared as well. Since all these parameters are controlled both by the dot radii and by the gate voltages, it is rather difficult to give quantitative estimates in a general form, but such estimates may be made numerically for a specific form of the dot, based, e.g., on self-consistent calculations of the charge distribution presented in Ref. 24 for a fork (ratchet) and triangular geometry of TQD's.

One should be aware that it is hardly possible to realize experimentally the ideal mirror symmetry in such a complicated object as a triple quantum dot. In the best case two side dots may be considered as nearly identical, so that the mirror reflection is only an approximately symmetry operation. Slightly violated mirror symmetry should result in a weak admixture of a state $|D_u\rangle$ to $|D_g\rangle$ and vice versa in the case $N=3$. The same is valid for the intermixture of the states E_{Db} and E_{Dn} in the case $N=1$. Both crossover effects described by the flow diagrams of Figs. 2 and 5 are relatively robust against this symmetry violation. In perfectly symmetric cases the Kondo effect is completely forbidden for the ground state E_{Du} in former state and the ground state E_{Dn} in the latter case. If the mirror symmetry is weakly violated, then the ban is not strict, so the evolution of T_K shown in Figs. 3 and 6 is not that sharp, but the crossovers in tunnel conductance shown in Figs. 4 and 7 are still observable. Of course, if the symmetry violation is strong and the matrix elements $\langle D_u|W|D_g\rangle$ and $\langle D_n|W|D_b\rangle$ are comparable with the distance between the corresponding levels far from the crossing points in the Haldane flow diagrams, the crossovers will be completely smeared. These matrix elements, which are controlled by the rotation angle θ, may be easily found by means of Eqs. (5) and (19), respectively [see also the discussion below Eq. (29)].

We have found in this study that the TQD with mirror symmetry at odd electron occupation $N=1,3$ possesses properties which were observed earlier only in dots with even occupation $N=2$. In particular, the Kondo tunneling may be absent in the ground spin-doublet state of the TQD due to special symmetry properties of the wave function (odd $l-r$ symmetry in case of $N=3$ and empty outer shell in case of $N=1$). The involvement of the low-lying Kondo-active spin doublet results in a two-stage Kondo screening reminiscent of that found in quantum dots with occupation $N=2$ where the spin excitation spectrum is formed by the singlet-triplet pair.[13] Other interesting possibilities now open due to the resonance valence bond structure of the electron wave function (19) in the case of a partially occupied inner shell in fork geometry with $N=1$. In particular the "pendulum effect"[14,15] perceived in TQD's with even occupation $N=2,4$ may be exploited in this type of TQD as well.

The transformation of the ZBA into the FBA under changing gate voltage is a special manifestation of a general phenomenon, known as the "critical phase transition," where the symmetry of the ground state changes as a function of control parameter. A similar effect should be observed in planar and double quantum dots[20] with even occupation where the singlet-triplet crossover may occur with changing gate voltage or in transition-metal molecular complexes.[25] In the latter case local phonons are essentially involved in this transition.[26]

ACKNOWLEDGMENTS

This work was partially supported by grant from the Israel Science Foundation (ISF) and the Deutsche Israel Project (DIP).

[1] K. Kikoin, M. N. Kiselev, and Y. Avishai, in *Nanophysics, Nanoclusters, Nanodevices* (Nova Science, New York, 2006), Chap. 2.

[2] L. I. Glazman and M. Pustilnik, in *Nanophysics: Coherence and Transport*, edited by H. Bouchiat *et al.* (Elsevier, Amsterdam, 2005), p. 427.

[3] C.-S. Neumann and P. Fulde, J. Chem. Phys. **94**, 3011 (1991).

[4] K. Kikoin and Y. Avishai, Phys. Rev. Lett. **86**, 2090 (2001); Phys. Rev. B **65**, 115329 (2002).

[5] K. Kang, S. Y. Cho, J-J. Kim, and S-C. Shin, Phys. Rev. B **63**, 113304 (2001); Y. Takazawa, Y. Imai, and N. Kawakami, J. Phys. Soc. Jpn. **71**, 2234 (2002).

[6] Y. Oreg and D. Goldhaber-Gordon, Phys. Rev. Lett. **90**, 136602 (2003).

[7] M. Pustilnik, L. Borda, L. I. Glazman, and J. von Delft, Phys. Rev. B **69**, 115316 (2004).

[8] T. Kuzmenko, K. Kikoin, and Y. Avishai, Phys. Rev. Lett. **89**, 156602 (2002); Phys. Rev. B **69**, 195109 (2004).

[9] N. J. Craig, J. M. Taylor, E. A. Lester, C. M. Marcus, M. P. Hanson, and A. C. Gossard, Science **304**, 565 (2004).

[10] P. Simon, R. Lopez, and Y. Oreg, Phys. Rev. Lett. **94**, 086602 (2005); M. G. Vavilov and L. I. Glazman, *ibid.* **94**, 086805 (2005); T. Tzen Ong and B. A. Jones, cond-mat/0602223 (unpublished).
[11] L. I. Glazman and M. E. Raikh, JETP Lett. **47**, 452 (1988).
[12] F. D. M. Haldane, Phys. Rev. Lett. **40**, 416 (1978).
[13] D. Giuliano and A. Tagliacozzo, Phys. Rev. Lett. **84**, 4677 (2000); M. Eto and Yu.V. Nazarov, *ibid.* **85**, 1306 (2000); M. Pustilnik and L. I. Glazman, *ibid.* **87**, 216601 (2001); W. Hofstetter and G. Zaránd, Phys. Rev. B **69**, 235301 (2004).
[14] D. S. Saraga and D. Loss, Phys. Rev. Lett. **90**, 166803 (2003).
[15] K. Le Hur, P. Recher, E. Dupont, and D. Loss, cond-mat/0510450 (unpublished).
[16] L. Borda, G. Zaránd, W. Hofstetter, B. I. Halperin, and J. von Delft, Phys. Rev. Lett. **90**, 026602 (2003).
[17] R. Sakano and N. Kawakami, Phys. Rev. B **72**, 085303 (2005).
[18] T. Kuzmenko, K. Kikoin, and Y. Avishai, Physica E (Amsterdam) **29**, 334 (2005); Phys. Rev. Lett. **96**, 046601 (2006).
[19] G. Zaránd, A. Brataas, and D. Goldhaber-Gordon, Solid State Commun. **126**, 463 (2003); B. Lazarovits, P. Simon, G. Zaránd, and L. Szunyogh, Phys. Rev. Lett. **95**, 077202 (2005); K. Ingersent, A. W. W. Ludwig, and I. Affleck, *ibid.* **95**, 257204 (2005).
[20] M. N. Kiselev, K. A. Kikoin, and L. W. Molenkamp, Phys. Rev. B **68**, 155323 (2003).
[21] A. Kaminski, Yu. V. Nazarov, and L. I. Glazman, Phys. Rev. B **62**, 8154 (2000).
[22] J. Paaske, A. Rosch, J. Kroha, and P. Wölfle, Phys. Rev. B **70**, 155301 (2004); A. Rosch, J. Paaske, J. Kroha, and P. Wölfle, J. Phys. Soc. Jpn. **74**, 118 (2005).
[23] A. Vidan, R. M. Westervelt, M. Stopa, M. Hanson, and A. C. Gossand, Appl. Phys. Lett. **85**, 3602 (2004).
[24] M. Stopa, Phys. Rev. Lett. **88**, 146802 (2002); M. Stopa, A. Vidan, T. Hatano, S. Tarucha, and R. M. Westervelt, cond-mat/0507591 (unpublished).
[25] K. Kikoin, M. N. Kiselev, and M. R. Wegewijs, Phys. Rev. Lett. **96**, 176801 (2006).
[26] M. N. Kiselev, M. R. Wegewijs, and K. Kikoin (unpublished).
[27] M. Avinun-Kalish, M. Heiblum, O. Zarchin, D. Mahalu, and V. Umansky, Nature (London) **436**, 529 (2005).